

Conducting polyaniline-graphene oxide fibrous nanocomposites: preparation, characterization and simultaneous electrochemical detection of ascorbic acid, dopamine and uric acid

Cite this: DOI: 10.1039/c3ra42322k

P. Manivel,^a M. Dhakshnamoorthy,^b A. Balamurugan,^a N. Ponpandian,^a D. Mangalaraj^a and C. Viswanathan^{*a}

Polyaniline/graphene oxide (PANI-GO) fibrous nanocomposites have been prepared and the electrochemical catalytic activity towards the electro-oxidation of ascorbic acid (AA), Dopamine (DA) and Uric acid (UA) has been investigated. The nanocomposites were synthesized *via an in situ* chemical polymerization method. The morphology, composition, thermal and electrochemical properties of the resulting nanocomposites were characterized by scanning electron microscopy, X-ray diffraction, Raman spectroscopy, FT-IR spectroscopy, thermo gravimetric analysis and cyclic voltammetry. The catalytic behavior of PANI-GO nanocomposite modified glassy carbon electrode (GCE) towards AA, DA and UA has been investigated by cyclic voltammetry (CV), differential pulse voltammetry (DPV). The PANI-GO/GCE showed excellent catalytic activity towards electrochemical oxidation of AA, DA and UA compared to the bare GCE. The electrochemical oxidation signal of AA, DA and UA are well separated into three distinct peaks with peak potential separation of 343 mV, 145 mV and 488 mV between AA-DA, DA-UA and AA-UA respectively in CV studies and the corresponding peak potential separation in DPV mode are 320 mV, 230 mV and 550 mV. Under the optimized DPV experimental conditions, the peak current of AA, DA and UA give linear response over the range of 25–200 μM ($R^2 = 0.9955$), 2–18 μM ($R^2 = 0.9932$) and 2–18 μM ($R^2 = 0.9902$) with detection limit of 20 μM , 0.5 μM and 0.2 μM at $S/N = 3$, respectively. The attractive features of PANI-GO provide potential applications in the simultaneous detection of AA, DA and UA. The excellent electrocatalytic behavior of PANI-GO may lead to new applications in electrochemical analysis.

Received 10th May 2013,
Accepted 29th May 2013

DOI: 10.1039/c3ra42322k

www.rsc.org/advances

Introduction

Ascorbic acid, dopamine and uric acid are compounds of great biological and chemical interest and play a potential role in the metabolic system of human body.^{1,2} Ascorbic acid (AA) is commonly used in large scale as an antioxidant in food, animal feed, pharmaceutical formulation and cosmetic applications.³ Dopamine (DA) is a neurotransmitter and plays a very important role in the function of central nervous, renal, hormonal and cardiovascular systems.⁴ Uric acid (UA) is the major final product of urine catabolism in human body. In a healthy human, the normal level of UA in urine is in milli molar range whereas in serum it is in micro molar range.⁵ Detection and quantification of AA, DA and UA are important in diagnosis, monitoring, prevention and treatment of certain

diseases such as cancer, diabetes mellitus, hepatic disorders, schizophrenia, Parkinson, hyperuricaemia, pneumonia and gout.^{2,6–9}

However, electrochemical determination of these species based on anodic oxidation has a disadvantage of overlapping oxidation peaks that is obtained at solid electrodes. At present, various modified electrodes, such as poly(acid chrome blue K) modified glassy carbon electrode,¹⁰ single-walled carbon nanohorn modified glassy carbon electrode,¹¹ chitosan-graphene modified glassy carbon electrode,² hollow nitrogen-doped carbon microsphere modified glassy carbon electrode,¹² iron ion doped natrolite zeolite-multiwall carbon nanotube modified glassy carbon electrode¹³ and graphene oxide-polyaniline composite modified electrode,¹⁴ *etc.* have been attempted to solve the problems encountered in simultaneous determination of AA, DA and UA. However, development of new materials for simultaneous electrochemical determination of various compounds is still one of the most attractive subjects which researchers strive to accomplish.

^aDepartment of Nanoscience and Technology, Bharathiar University, Coimbatore-641 046, Tamil Nadu, India. E-mail: viswanathan@buc.edu.in; Fax: +91 422 2422387; Tel: +91 422 2428422

^bPolymer Nanotechnology centre, B.S.Abdur Rahman University, Chennai-600 048, Tamil Nadu, India

Conducting polymers are in use as an alternative to metal oxide materials for potential applications. Among the conducting polymers polyaniline (PANI) has become one of the technologically important conducting polymers, because of its relatively low cost, simple synthesis, good optical and electrical properties with excellent environmental stability.^{15–17} It also has electrochemical properties and finds potential applications for electronic, optical devices,^{18–22} such as light emitting diodes, sensors, electronic circuit boards, and bioelectrochemical sensing.^{17,22} However, PANI was reported to be less sensitive to bio molecules. This issue could be alleviated by introducing suitable functional groups into polymer backbone or conjugating PANI with others materials which are sensitive to neurotransmitter DA,^{14,23} such as metal nanoparticles and carbon nanomaterials, *etc.* Feng *et al.* have synthesized PANI/Au composite hollow sphere and studied the bioelectrocatalytic activity in the oxidation of DA.²⁴ Ali *et al.* have reported the preparation of self-doped PANI/Carbon nanotube composites for the sensitive and selective detection of DA.²⁵

In recent years, numerous reports have been published on graphene oxide and graphene. Graphene, a flat monolayer of hexagonally arrayed sp²-bonded carbon atoms tightly packed into a two-dimensional (2D) honeycomb lattice, has been the major focus of recent research due to its excellent electrical, mechanical, thermal and optical properties,^{26,27} leading to their potential applications in many different areas such as nanoelectronics, super capacitor, gas sensors and chemical sensors^{28–31} and also many graphene based electrode materials and nanocomposites have been developed for sensing biomolecules such as glucose,³² nicotinamide adenine dinucleotide,³³ dopamine and mixture of AA, DA and UA.^{5,31} Researchers particularly endeavor to prepare functionalized graphene layer with enhanced solubility, dispersibility, mechanical and electrochemical properties. Ping *et al.* have reported selective, sensitive and simultaneous detection of AA, DA and UA using high-performance screen-printed electrode.³ The potential separation in this analysis indicates the superior selectivity of this system. Wu *et al.* have reported an electrochemical method on selective detection of DA by porphyrin-functionalized graphene.³⁴ The simultaneous electrochemical detection of mixture of bio-molecules (AA, DA and UA) using chitosan-graphene modified electrode system was reported by Han *et al.*²

Furthermore, graphene oxide (GO) and reduced graphene oxide (RGO) have also been intercalated or used to make composites with PANI through *in situ* chemical polymerization and *in situ* anodic electrochemical polymerization to prepare PANI-GO and PANI-RGO nanocomposites for potential application in energy storage.^{35–38} However, the electrocatalytic activities of both graphene oxide and graphene with polyaniline nanocomposites have very rarely been analyzed. Very recently, Bai *et al.*³⁹ reported the electrocatalytic activity of functionalized graphene sheets incorporating sulfonated PANI electroactive composite towards AA and Bao *et al.*¹⁴ reported graphene oxide-templated polyaniline microsheet towards simultaneous electrochemical analysis of AA, DA and UA.

However, to best of our knowledge, there are no reports on highly selective, sensitive and simultaneous detection of AA, DA and UA based on PANI-GO and PANI-RGO nanocomposite modified electrodes in their ternary mixture.

In this work, Polyaniline/graphene oxide (PANI-GO) fibrous nanocomposites were synthesized *via* an *in situ* chemical oxidation polymerization method. The PANI-GO fibrous nanocomposite electrocatalysts were drop coated on the glassy carbon electrode (GCE) to detect AA, DA and UA simultaneously with high selectivity and sensitivity.

Experimental

Materials

Natural graphite flakes (10 meshes) were purchased from Alfa Aesar. Aniline was purchased from Sd-fine chemical and was distilled under reduced pressure and kept below 0 °C before use. Ascorbic acid, dopamine and uric acid were obtained from Sigma-Aldrich. Sodium nitrate, sulfuric acid, hydrochloric acid, potassium permanganate, ammonium peroxydisulfate, Sodium hydroxide, potassium dihydrogen phosphate and sodium phosphate were obtained from Himedia chemicals and hydrogen peroxide obtained from Sd-fine chemicals. All the analytical-reagent grade chemicals were used without further purification. Phosphate buffer solution (PBS 0.05 M, pH 7) was prepared with potassium dihydrogen phosphate and sodium phosphate. All the aqueous solutions were prepared with double-distilled water.

Synthesis of graphene oxide (GO)

Graphene oxide was synthesized from natural graphite flakes by a modified Hummers method.³⁸ Graphite (1 g) and NaNO₃ (1 g) were mixed with 75 mL H₂SO₄ (95%) in a 250 mL flask. The mixture was stirred for 30 min on an ice bath. While maintaining vigorous stirring, potassium permanganate (3 g) was added to the suspension. The rate of addition was carefully controlled to keep the reaction temperature well below 20 °C. The ice bath was then removed, and the mixture was stirred at room temperature for 7 h. Additional potassium permanganate (3 g) was added in one portion, and stirring was continued for 12 h at room temperature. As the reaction progressed, the mixture gradually became the consistency of the mixture increased as the reaction progressed and the color turned light brown. At the end, 100 mL of deionized water was slowly added to the viscous mixture with vigorous agitation. The reaction temperature rapidly increased to 98 °C while the system color changed from brown to yellow and effervescence was observed. The dilute suspension was stirred for 12 h. Finally 20 mL of 30% H₂O₂ was added to the mixture. For purification, the mixture was washed by rinsing and centrifuging with 5% HCl and then washed with deionized (DI) water for several times. After drying under vacuum, the brown color graphene oxide (GO) was obtained.

Synthesis of polyaniline nanofibers (PANI)

Aniline was first distilled under vacuum to remove the oxidation impurities. The purified aniline (0.2 M) was

dissolved in 100 mL of 1 M HCl aqueous solution. While maintaining vigorous stirring at room temperature, the ammonium peroxydisulfate (0.25 M) in 50 mL of 1 M HCl aqueous solution was slowly added drop wise into the aniline solution. Polymerization was observed after complete addition when the characteristic green color of polyaniline emeraldine salt appeared. The mixture was allowed to stir at room temperature overnight. The precipitated polyaniline was collected by filtration and repetitively washed with double distilled water, ethanol and acetone successively until the filtrate became colorless and dried in vacuum oven at 60 °C overnight.

Synthesis of polyaniline-graphene oxide nanocomposites (PANI-GO)

Graphene oxide and polyaniline fiber nanocomposites were prepared by *in situ* polymerization of aniline in a suspension of graphene oxide in acidic solution. The weight ratio of aniline to graphene oxide was varied as 100 : 1, 100 : 2, 100 : 3, 100 : 4 and 100 : 5 and the resulting composites were named as PANI-GO1, PANI-GO2, PANI-GO3, PANI-GO4 and PANI-GO5, respectively. Typically, the graphene oxide was dispersed in 100 mL of 1 M HCl aqueous solution by bath sonicating for 1 h. Then 0.2 M aniline was dissolved in the dispersed GO containing acidic aqueous solution. While maintaining vigorous stirring at room temperature, ammonium peroxydisulfate solution, with a mole ratio to aniline of 1 : 2, in 1 M HCl was added drop wise into the resulting mixture. After about 5 min of addition, the aniline started to polymerize while the color of mixture changed into green. The mixture was stirred at room temperature overnight. The composites were collected by filtration and repetitively washed with double distilled water, ethanol and acetone successively until the filtrate became colorless and dried in vacuum oven at 60 °C overnight.

Characterization

A QUANTA 250 field emission scanning electron microscope (FE-SEM) was used to determine the morphology of the composites. The FT-IR spectra of the samples were recorded on a Thermo Nicolet is10-ATR mode FT-IR spectrometer by using KBr pellets to confirm the presence of functional groups. Raman spectra were recorded at ambient temperature on a Horiba Jobin-LabRam-HR UV spectrometer with Argon laser at an excitation wavelength of 514 nm. The electrochemical measurements including cyclic voltammetry were performed with an electrochemical work station CHI 1120A (CH instruments, USA). A conventional three-electrode cell was used, including Ag/AgCl (saturated KCl) electrode as the reference electrode, a platinum wire as the counter electrode and glassy carbon electrode (GCE, 3 mm in diameter) as the working electrode.

Preparation of PANI-GO modified electrode

The GCE surface was carefully polished to a mirror like finish in alumina slurries with 0.5 and 0.05 μm (mesh), successively. Afterwards, the electrode was washed thoroughly with excess amount of water and dried in ambient atmosphere. A certain amount of PANI-GO nanocomposite was ultrasonicated in

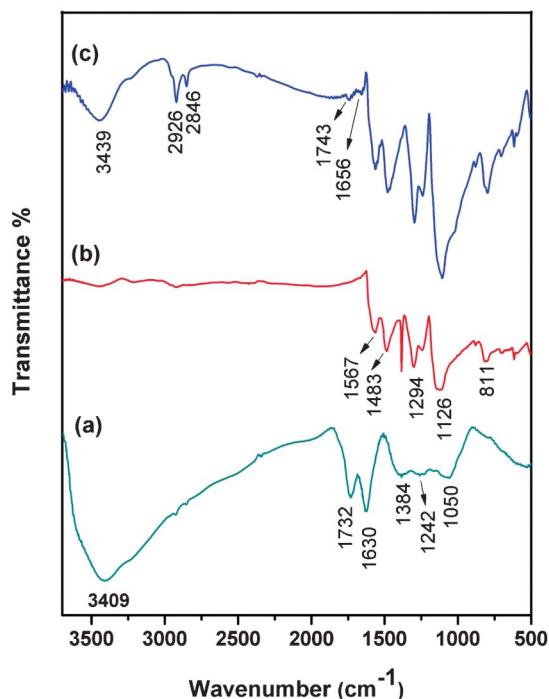


Fig. 1 FTIR spectra of (a) GO, (b) PANI and (c) PANI-GO nanocomposite.

distilled water to form a homogenous dispersion. Then 5 μL of the above solution was drop cast on the surface of a freshly polished GCE and dried at ambient atmosphere for 5 h.

Results and discussions

Structure, morphology and properties of PANI-GO nanocomposites

FTIR spectroscopy was used to characterize the *in situ* chemical polymerization of aniline on the GO sheets. Fig. 1 displays the typical spectra of oxidized GO, PANI, and PANI-GO nanocomposites. Fig. 1a, shows the presence of the oxygen-containing functional groups on GO. The bands at 1050, 1242, 1384, 1630 and 1732 cm^{-1} corresponds to the C–O–C stretching vibrations, C–OH stretching peak, O–H deformation of the C–OH group, C=C stretching mode and C=O stretching vibrations of the –COOH group, respectively. The broad and intense peak corresponding to the stretching vibrations of O–H at 3409 cm^{-1} indicates that the GO samples contain large quantity of adsorbed water molecules. These features suggest that graphene oxide is heavily oxidized and consists mainly –OH and other oxygen containing functional groups. As shown in Fig. 1b, the strong absorption peaks has been assigned to the stretching of quinonoid ring (C=N) appeared at 1567 cm^{-1} , benzenoid rings (C–C) appeared at 1483 cm^{-1} , The peak at 1387 cm^{-1} corresponds to C–N stretching in the neighborhood of a quinonoid ring. The band at 1294 cm^{-1} is assigned to the C–N stretch of a secondary aromatic amine. The aromatic C–H in-plane bending modes appeared at 1126 cm^{-1} and aromatic CH out-of-plane bending appeared at 811 cm^{-1} . As shown in

Fig. 1c, the FTIR spectrum of PANI-GO is almost the same as PANI (Fig. 1b). The absorption peaks of the amide group were observed at 1656 cm^{-1} for PANI-GO. This showed amidation between the carboxylic acids group of GO and the amino group of aniline and also, the absorption peak of C=O groups has red shifted to 1743 cm^{-1} from 1732 cm^{-1} of composites. These results indicate that the carboxylic groups on the edge region of GO have partially reacted with the amino group of the aniline monomer. The structure of the interface between GO and PANI features a combination of electrostatic interaction, hydrogen bonds and π - π interactions.³⁵ The characteristic peaks of PANI at 1567 and 1483 cm^{-1} manifests the presence of PANI in the PANI-GO composite. In addition, matching with Chen *et al.* reports, we also observed the reappearance of a band at 2926 cm^{-1} for the CH_2 groups (Fig. 1c) implying a restoration of the carbon basal planes on account of reduction by hydrogen.⁴⁰

Fig. 2 shows, the Raman spectra for the developed PANI-GO nanocomposite as well as for pure PANI fiber and GO layer. In the Raman spectrum of GO layer (Fig. 2a), the two intense bands at 1357 cm^{-1} and 1595 cm^{-1} have been assigned to D band and G band respectively. The G band assigned to the first order scattering of the E_{2g} phonon of GO represent the in-plane bond stretching vibration of sp^2 -bonded carbon atoms in a 2D hexagonal lattice. The D band is associated with the breathing mode of K-point phonons of A_{1g} symmetry with vibration of carbon atoms with dangling bonds in plane terminations of disordered graphite.^{41,42} In the Raman spectrum of pure PANI nanofiber (Fig. 2b), the characteristic bands appear at 1585 and 1347 cm^{-1} , which are assigned to the C=C stretching vibration of the quinonoid ring and C-H bending vibration of benzene ring in the backbone of PANI, respectively. The band at 1046 cm^{-1} is attributed to symmetrical C-H in-plane bending vibrations.⁴³ The peaks

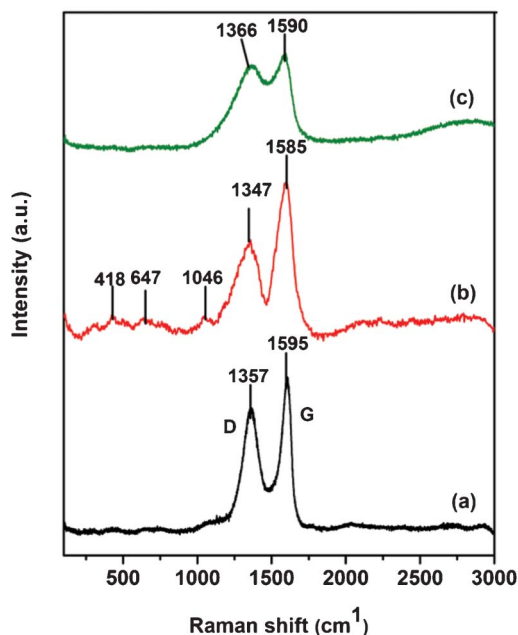


Fig. 2 Raman spectra of (a) GO, (b) PANI and (c) PANI-GO nanocomposite.

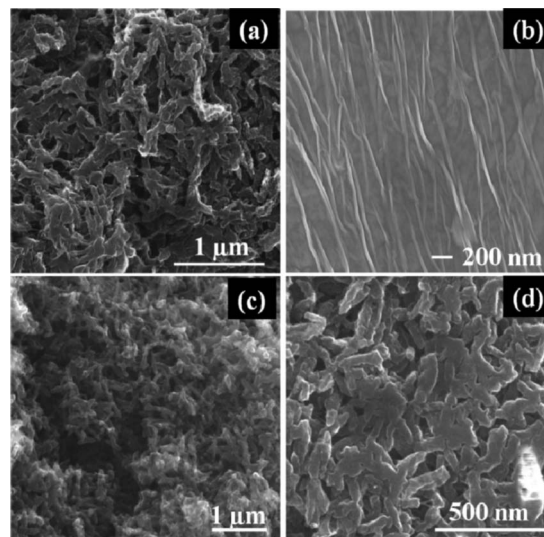


Fig. 3 SEM images of (a) PANI, (b) GO and (c, d) PANI-GO nanocomposite.

observed at 647 cm^{-1} can be attributed to bipolaronic benzene ring deformations, while the peak related to the polaronic C-N-C torsion was obtained at 418 cm^{-1} ref. 35,44. In the Raman spectrum of PANI-GO nanocomposite (Fig. 2c), the D band becomes broad during the *in situ* polymerization process, implying in-plane bending vibration of C-H molecules overlapped in the D band of GO layer. In addition, the composites presented a shift of D and G bands towards higher wavelength when GO was introduced into the PANI. This is probably due to the doping of carboxyl group of graphene oxide to PANI backbone and π - π interaction between PANI and GO sheets.³⁵

To visually learn the dimensional self-construction of the prepared nanocomposite, the surface morphologies and shape of the PANI, GO and PANI-GO are shown in Fig. 3. The pure PANI shows short agglomerated fibers with some granular particles in the order of ~ 150 to 200 nm (Fig. 3a). The GO sheets was composed of a layered structure are stacks wrinkled (Fig. 3b), while the PANI-GO composites were composed of smooth surface fibers. Since the uniform PANI nanofibers have been grown on the surface of the GO nanosheets in the order lower than $\sim 100\text{ nm}$. In analyzing the morphology of the PANI-GO nanocomposite (Fig. 3b), it is important to take into consideration the electron transport properties of both GO and aniline monomer in order to determine the molecular binding mechanism.⁴⁴ The strong affinity between the negatively charged carboxyl group and the positively charged amine nitrogen groups makes the PANI fibers firmly attach with the GO nanosheets.⁴² The aniline monomer is first adsorbed onto the surface of the GO nanosheets during the formation of PANI nanofiber on GO nanosheets due to electrostatic attraction. Oxidation of aniline by oxidizing agent gives a nanostructured product shown in Fig. 3. This result was reported earlier by Sadek *et al.*⁴⁵ Hence, the GO nanosheets can be considered as a support material providing a large number of active nucleation sites for PANI growth.⁴⁶

TGA and DTG studies were carried out to study the thermal stability of PANI, GO and PANI-GO nanocomposites shown in

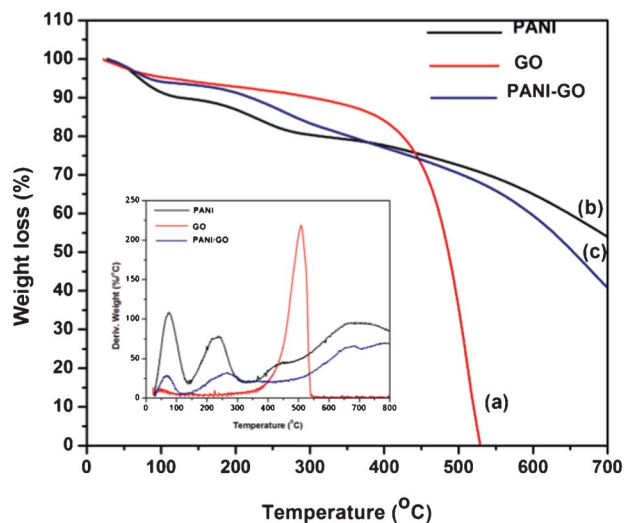


Fig. 4 TGA curve of (a) GO, (b) PANI and (c) PANI-GO nanocomposite. Inset: DTG curves of GO, PANI and PANI-GO nanocomposite.

Fig. 4. As shown in Fig. 4a, GO first starts to lose weight upon heating from 50 °C to 150 °C owing to the evaporation of water present between the layers in GO; a second major weight loss occurs at about 300 °C which is due to the decomposition of oxygen containing functional groups (such as C–OH, C–O–C, COOH) producing CO₂, CO and H₂O which are removed from the GO nanosheets. For the pure PANI (Fig. 4b), the gradual weight loss in the temperature range from 70 °C to 200 °C shows 20% mass loss which is due to dehydration and deprotonation of the PANI.⁴⁷ However, a rapid change in major weight loss of 40% takes place in the range 230 °C to 650 °C, which corresponds to the degradation and decomposition of PANI at different polymerization stage. In PANI/GO nanocomposite (Fig. 4c), the slow weight loss near 70 °C to 260 °C can be attributed to the loss of co-intercalated water molecules and the release of co-intercalated HCl. After 260 °C, major weight loss occurs due to decomposition of the PANI in the nanocomposite. Finally the weight loss of 50% takes place in the range, at about 650 °C for GO-based PANI nanocomposite. In general, the thermal stabilities of the PANI-GO nanocomposite are greater than that of the GO presumably because of the elimination of the OH groups and the incorporation of PANI chain molecules.⁴⁰ Also, the percentages of major weight loss of the molecules corresponding to the temperature are shown in inset Fig. 4.

Electrochemical characteristics of PANI/GO nanocomposite modified GCE electrodes

Following previous report⁴⁸ the working electrodes were prepared by casting a Nafion-impregnated composite sample onto a glassy carbon electrode. Fig. 5 compares the CV curve of the bare GCE, PANI and PANI-GO nanocomposite modified GC electrodes at a scan rate of 20 mV s⁻¹ within the potential range from -0.2 to +0.8 V vs. Ag/AgCl in the aqueous solution of 1 M H₂SO₄ electrolyte. The weights of the active materials

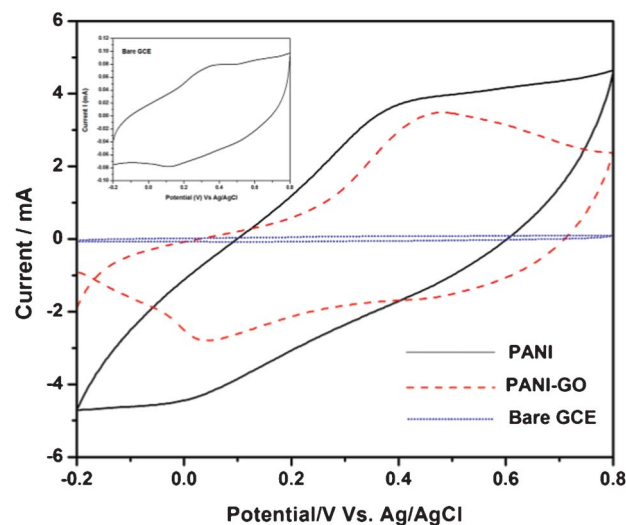


Fig. 5 Cyclic voltammogram curves of bare GCE, PANI and PANI-GO nanocomposite.

(PANI and PANI-GO) were controlled to be the same on each modified electrode.

Each CV curve is nearly rectangular in shape, indicating good charge propagation within the electrode. A couple of oxidation and reduction peaks are observed from the CV curve of PANI, corresponding to transition of leucoemeraldine/polaronic emeraldine form and Faradic transformation of emeraldine/permanganine.^{38,49}

It is clear from Fig. 5 that the CV curve current densities of the PANI nanofiber modified GC electrode is higher than those of the PANI-GO nanocomposite modified GC electrode and bare GC electrode. The GO containing nanocomposite (PANI-GO) shows typically a couple of well defined oxidation and reduction peaks when compared to pure PANI nanofiber (Fig. 5). This, suggests that the more oxygen containing functional groups of GO nanosheets in the composite contribute a little to the current density, and the total pairs of oxidation and reduction peaks are well defined by the Faradic process (cathodic and anodic) than the conducting PANI nanofiber. This is mainly due to the PANI nanofiber grown on the surface of GO nanosheets improve the charge transfer between the active materials and GC electrode. Therefore, the electrochemical catalytic behavior of PANI was further improved by intercalation with GO sheets.

The PANI-GO nanocomposite modified GC electrode was also observed with enhanced electrochemical stability. Fig. 6A reveals that in the CV curve of PANI modified electrode, current decreases significantly with increase in the number of cycles. The electrode current decreases by 0.8 mA at 100th cycle and by 1.2 mA at 500th cycle from first cycle. On the other hand the CV curve of PANI-GO nanocomposite modified GC electrode was almost the same as the first cycle as shown in Fig. 6B. Also, there is only a slight change in the CV curve of PANI-GO nanocomposite modified GC electrode after 500th cycle. Based on the electrochemical properties described above, it can be concluded that the small amount (1–5%) of

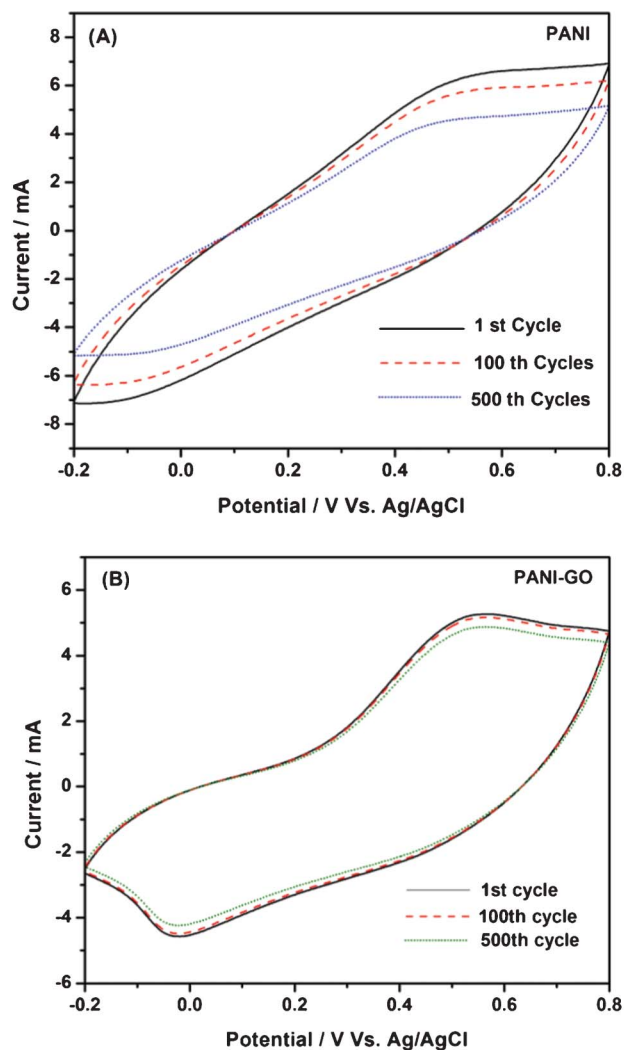


Fig. 6 Cyclic voltammogram curves of (A) PANI and (B) PANI-GO nanocomposite.

GO introduced into the PANI can greatly improve the electrochemical stability of the PANI nanofiber.

Electrocatalytic oxidation characteristics of AA, DA and UA at PANI-GO modified GCE

Fig. 7 illustrates the cyclic voltammetric responses of the bare GC electrode and PANI-GO nanocomposite modified GC electrode in 0.05 M PBS solution (pH 7.0) containing 1 mM AA, 1 mM DA and 1 mM UA within the potential window of -0.2 – 0.8 V and at scan rate of 50 mV s^{-1} . As can be seen in Fig. 7A, AA, and UA shows irreversible oxidation peaks at 514 and 299 mV, respectively. DA shows quasi-reversible electrochemical behavior with the anodic and cathodic peak potential at 399 mV and 300 mV at the bare GC electrode. It seems that the separation of the anodic peak potentials for these three molecules is not enough to obtain good selectivity at the bare GC electrode.

For the PANI-GO nanocomposite modified GC electrode as shown in Fig. 7B, the corresponding anodic oxidation peak

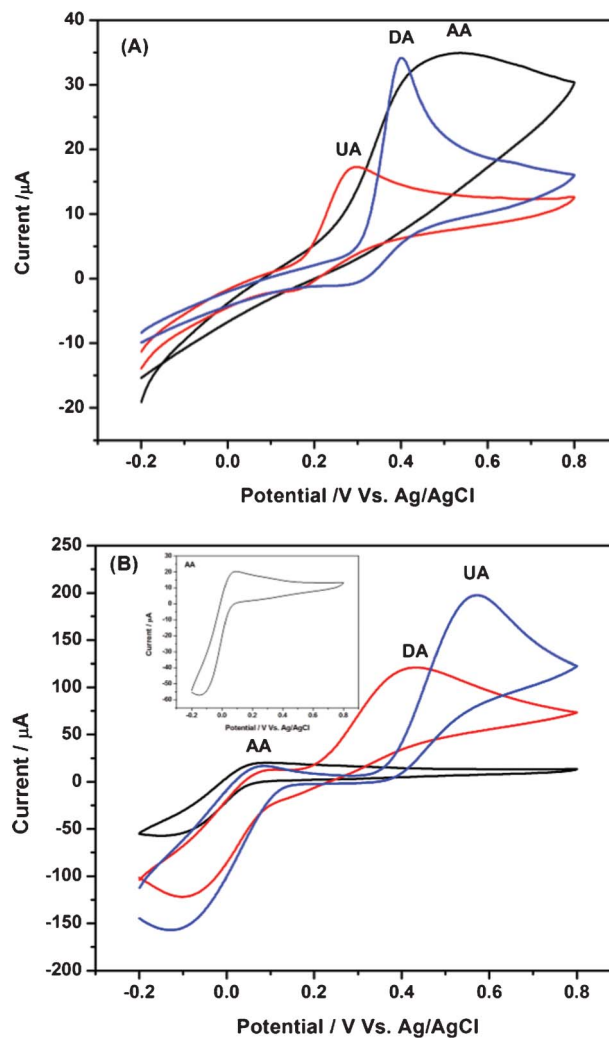


Fig. 7 Cyclic voltammogram curves of 1.0 mM AA, 1.0 mM DA and 1.0 mM UA at bare GCE (A) and PANI-GO/GCE (B) in 0.05 M (pH 7.0) PBS. Scan rate: 50 mVs^{-1} .

potential of AA is negatively shifted to 82 mV and oxidation peak potential of DA and UA are a positively shifted to 425 mV and 596 mV. The difference between AA and DA peak potentials is above 300 mV, which is enough to characterize AA and DA. The current densities observed at PANI-GO nanocomposite modified GC electrode are more or less six times higher than that of the bare GC electrode. These results suggest that the electron transfers for the oxidation of AA, DA and UA at the PANI-GO nanocomposite is much easier, due to the increased surface area. Such an improvement in electron transfer kinetics could be attributed to the doping of carboxylic group of graphene oxide to PANI backbone and π - π interaction between PANI and GO sheets which may offer some favorable sites for transferring the electrons to biomolecules and would accelerate the electron transfer between electrode surface and electroactive molecules.⁵⁰

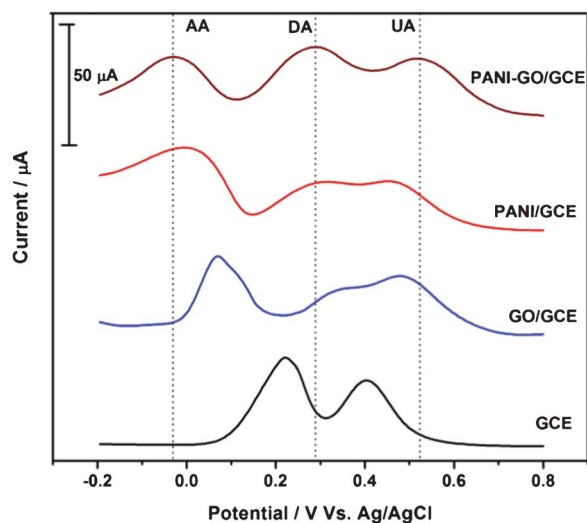
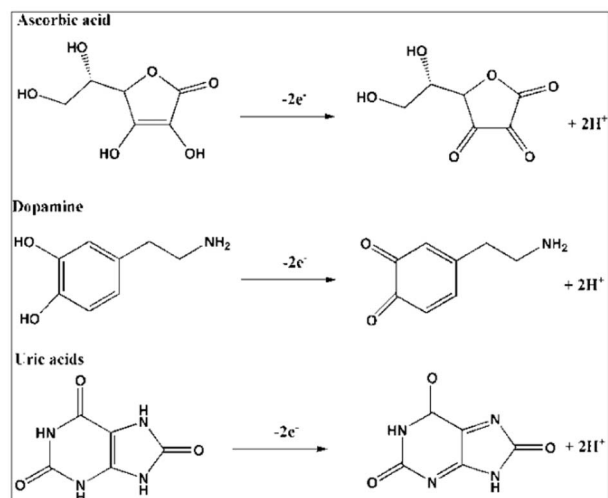


Fig. 8 DPV curves at bare GCE, GO/GCE, PANI/GCE and PANI-GO/GCE in 0.05 M (pH 7.0) PBS containing ternary mixture of 1 mM AA, 1 mM DA and 1 mM UA. DPV settings: step potential: 5 mV; amplitude: 60 mV; pulse width: 0.05 s; sample width: 0.01 s and pulse period: 0.2 s.

Electrocatalytic oxidation characteristics of AA, DA and UA in a ternary mixture

The electrocatalytic activity of PANI-GO nanocomposite modified GC electrode towards the oxidation of these three bio-molecules in a mixture is also investigated by the sensitive technique of differential pulse voltammetry (DPV). Fig. 8 shows the DPV peaks of ternary mixture of AA, DA and UA at bare GCE, GO/GCE, PANI/GCE and PANI-GO/GCE. At the bare GC electrode, the electro-oxidation of AA and DA molecules is completely overlapped and presents a broad overlapped peak (at 222 mV) so that simultaneous determination of these three molecules is impossible. On the contrary, well defined DPV oxidation peaks were observed at PANI-GO/GCE with peak potential value of -30 mV, 290 mV and 520 mV for AA, DA and UA, respectively. The separation of electro oxidation peak potential for AA-DA, DA-UA and AA-UA are 320 mV, 230 mV and 550 mV, respectively. The large separation of the peak potentials reveals that PANI-GO nanocomposite with higher electrocatalytic activity can be used to construct electrochemical sensor for selective determination of AA, DA and UA in the presence of the other two molecules, or simultaneous detection of them in their ternary mixture. The plausible mechanisms (Scheme 1) behind the simultaneous detection of AA, DA and UA with wide potential separation of PANI-GO nanocomposite modified GC electrodes can be explained as follows. The molecular structure of DA and AA are different from each other. The improved oxidation could be due to the π - π interaction between phenyl structure of DA and PANI-GO nanocomposite and the hydrogen bonds formed between hydroxyl or amine groups of DA and nitrogen atom within nanocomposite fiber.⁵¹ Although the π - π interaction between penta-heterocyclic system of AA and PANI-GO nanocomposite is weak, the presence of cationic emeraldin salt provide a significant electrostatic attraction to negatively charged AA



Scheme 1 Schematic representation of the simultaneous electrocatalytic oxidation of AA, DA and UA.

and UA, but rejection to positively charged DA due to the charge characters of AA ($pK_a = 4.1$), DA ($pK_a = 8.8$), and UA ($pK_a = 3.7$).¹⁴ Both the CV and DPV measurements demonstrate that PANI-GO nanocomposite possess good electrocatalytic activity towards the oxidation of these three molecules.

In the control experiment, only one distinct anodic peak of AA is observed in GO/GC electrode at 69 mV and two small intense anodic peaks observed at about 340 mV and 480 mV indicating that the oxidation peaks of DA and UA cannot be distinguished from each other in GO/GCE. It seems that it is possible for PANI/GCE to differentiate individual analyte species. However, compared to PANI-GO/GCE, the DA and UA oxidation peak is much lower, and the DA-UA peak separation is smaller. PANI-GO has electrochemical activity in neutral solution, and its electrochemical activity has been greatly enhanced than the PANI fibers. The possible reason for this preferable electrocatalytic behavior may be attributed to the fiber structure of nanocomposite, which provides larger surface area thereby enhancing the sensing signal and accelerating the electron transport which is due to the strong π - π stacking between PANI and GO.³⁹

Effects of the mass ratio of aniline/GO and pH on the electrochemical oxidation behavior of AA, DA and UA

Fig. 9 shows the different mass ratio of aniline to GO during the polymerization process on the DPV responses of AA, DA and UA in their ternary mixture at the PANI-GO nanocomposite modified GC electrode. The different mass ratios of aniline to GO chosen for analysis were 100 : 1, 100 : 2, 100 : 3, 100 : 4 and 100 : 5 and they were named as PANI-GO 1, PANI-GO 2, PANI-GO 3, PANI-GO 4 and PANI-GO 5 respectively. The anodic peak potentials for ternary mixture of these three molecules are well defined in the five ratios, and the PANI-GO 3 nanocomposite modified GC electrode obtained a large peak potential separations. The PANI-GO 3 modified GC electrode can effectively resolve the merged voltammetric peak into three well defined anodic oxidation peak at potential of about

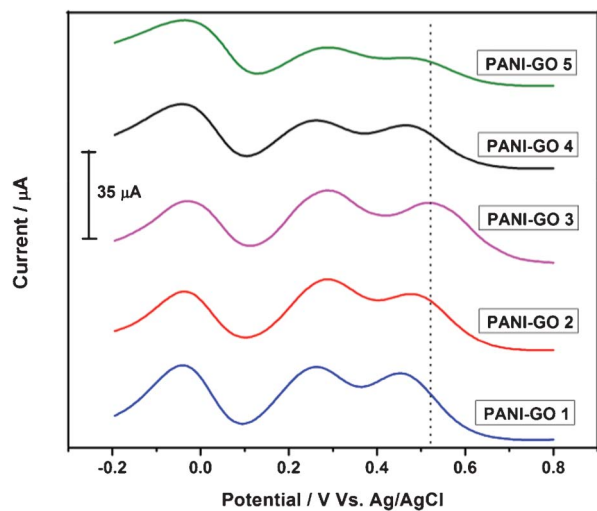


Fig. 9 DPV curves at PANI-GO/GCE in 0.05 M (pH 7.0) PBS containing ternary mixture of 1.0 mM AA, 1.0 mM DA and 1.0 mM UA. Different ratios of aniline to GO (mass ratio) during PANI-GO polymerization process. The ratios of aniline to GO in 100 : 1, 100 : 2, 100 : 3, 100 : 4 and 100 : 5. DPV settings: step potential: 5 mV; amplitude: 60 mV; pulse width: 0.05 s; sample width: 0.01 s and pulse period: 0.2 s.

–30 mV, 290 mV and 520 mV for AA, DA and UA, respectively. The separation of electro oxidation peak potential for AA-DA, DA-UA and AA-UA are 320 mV, 230 mV and 550 mV, respectively. These large anodic peak potential separations indicates that 100 : 3 aniline-GO ratio is a very suitable ratio for selective determination of AA, DA and UA in the presence of the other two molecules, or simultaneous detection of them in their ternary mixture.

The influence of solution pH on the peak current and peak potential of the electrocatalytic anodic oxidation of AA, DA and

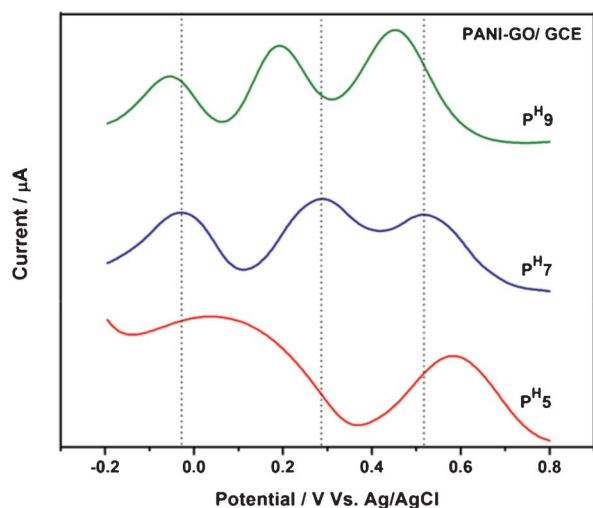


Fig. 10 DPV curves at PANI-GO/GCE in 0.05 M (pH 5.0, 7.0 and 9.0) PBS containing ternary mixture of 1.0 mM AA, 1.0 mM DA and 1.0 mM UA. DPV settings: step potential: 5 mV; amplitude: 60 mV; pulse width: 0.05 s; sample width: 0.01 s and pulse period: 0.2 s.

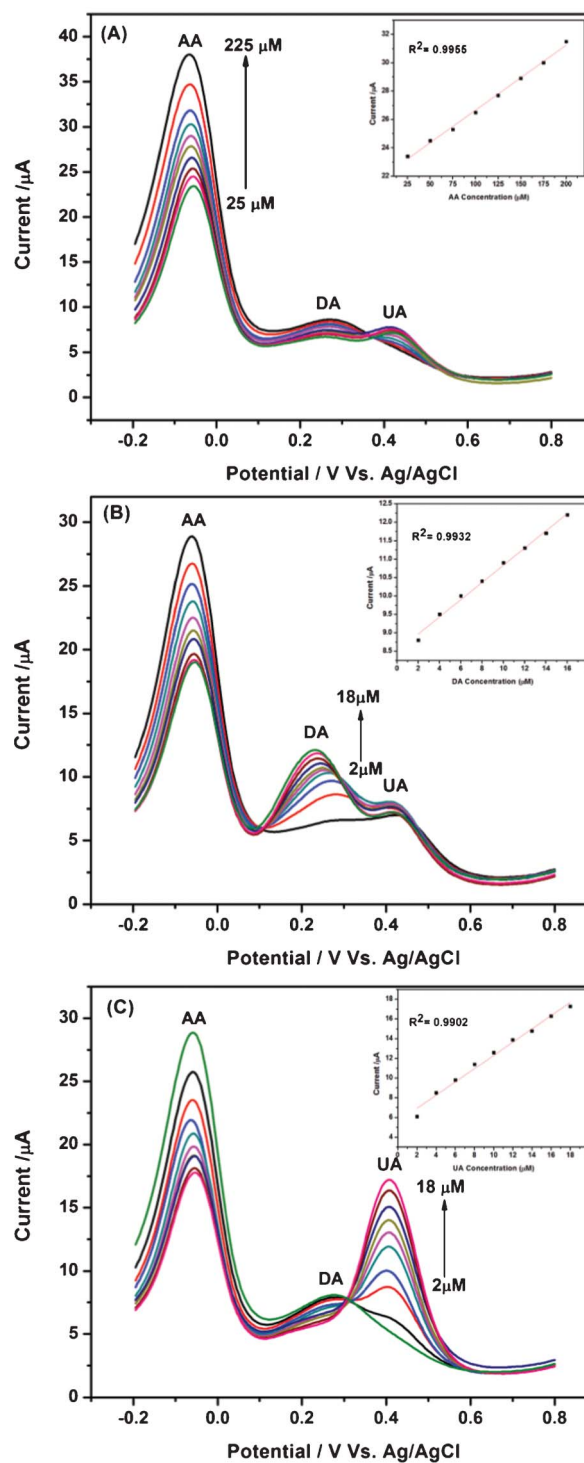


Fig. 11 DPVs at the PANI-GO/GCE in 0.05 M (pH 7.0) PBS containing 10 µM DA, 10 µM UA and different concentrations of AA (from inner to outer): 25, 50, 75, 100, 125, 150, 175, 200, 225 µM (A), containing 100 µM AA, 10 µM UA and different concentrations of DA (from inner to outer): 2, 4, 6, 8, 10, 12, 14, 16, 18 µM (B) and containing 100 µM AA, 10 µM DA and different concentrations of UA (from inner to outer): 2, 4, 6, 8, 10, 12, 14, 16, 18 µM (C). DPV settings: step potential: 5 mV; amplitude: 60 mV; pulse width: 0.05 s; sample width: 0.01 s and pulse period: 0.2 s. Inset: Plot of peak currents vs. sample concentrations.

Table 1 Comparison of the analytical performance of the different modified electrodes for the simultaneous determination of AA, DA and UA

Electrode materials	Linear range (μM)			Detection limit (μM)			Sensitivity ($\mu\text{A } \mu\text{M}^{-1}$)			Potential separation (mV)			Ref.
	AA	DA	UA	AA	DA	UA	AA	DA	UA	AA-DA	DA-UA	AA-UA	
Poly-ACBK	50-1000	1-200	1-120	1.0	0.5	0.5	0.002	0.147	0.007	193	166	359	10
SWCNH	30-400	0.2-3.8	0.06-10	5.0	0.06	0.02	0.020	3.5	5.6	211	152	363	11
CG/GCE	50-1200	1.0-24	2.0-45	50	1.0	2.0	0.012	0.375	0.45	165	90	255	2
HNCMS/GC	100-1000	5-70	3-30	0.91	0.02	0.04	0.027	0.93	0.59	136	212	248	12
MWCNT-FeNAZ/GCE	20-355	65-260	6-25	1.11	1.05	0.03	—	—	—	270	150	430	13
GO-PANI/GCE	150-850	2-14	2-16	50	0.5	1.0	0.04	1.3	0.7	250	190	440	14
PANI-GO/GCE	25-200	2-18	2-18	20	0.5	0.2	0.92	2.0	2.2	320	230	550	Our work

UA at the PANI-GO nanocomposite was also investigated by DPV techniques in the pH ranging from 5 to 9 as shown in Fig. 10. The anodic oxidation peaks of AA and DA were overlapped, when the solution pH was below 6. It is clear that with the increase in solution pH between 7 and 9, the anodic oxidation peak potential of AA, DA and UA shifted negatively. This indicates, protons are directly involved in the overall electrochemical oxidation reactions, *i.e.*, the oxidation reaction occur *via* electron transfer step followed by protonation process.⁵² Furthermore, it is evident that the large separation of the peak potential for AA-DA and DA-UA are obtained at pH 7. Therefore, individual or simultaneous determination of AA, DA and UA from their ternary mixture can be realized at the PANI-GO nanocomposite modified GC electrode in a wide pH range. Based on the peak potential separation and detection sensitivity, the buffer solution of pH 7 was selected in our measurements.

Simultaneous determination of AA, DA and UA

Simultaneous determination of AA, DA and UA at the PANI-GO modified GC electrode was carried out by DPV in their ternary mixture, when the concentration of one species changed while other two species remained constant. As shown in Fig. 11, the electro oxidation peak current of AA, DA, or UA increases linearly with the increase of the biomolecule concentration. The corresponding linear range for AA, DA and UA determination are 25 to 200 μM ($R^2 = 0.9955$), 2 to 18 μM ($R^2 = 0.9932$) and 2 to 18 μM ($R^2 = 0.9902$) with detection limit of 20 μM , 0.5 μM and 0.2 μM at $S/N = 3$, respectively. And the relative standard deviation (*RSD*) obtained were 4.81%, 4.03% and 4.92% for AA, DA, UA, respectively. Comparing the data shown in the previous literatures (Table 1), improved performance for the simultaneous determination of AA, DA and UA can be achieved using the PANI-GO/GCE. To best of our knowledge, direct electrochemical determination of AA, DA and UA with such a high sensitivity and large potential separation is rarely reported. This PANI-GO nanocomposite with unique structural and electrocatalytic properties is a promising candidate for the fabrication of sensitive and selective biosensors.

Conclusions

Polyaniline-graphene oxide fibrous nanocomposites have been successfully synthesized by *in situ* polymerization. The fibrous structure of PANI-GO nanocomposite shows excellent electro-

catalytic activity towards the oxidation of AA, DA and UA. Furthermore, in AA, DA and UA ternary mixture, three well defined peaks at about -30 mV, 290 mV and 520 mV were obtained, which is ascribed to the π - π interaction and electrostatic attraction between the target biomolecules and PANI-GO nanocomposite. In addition, the electro oxidation of AA, DA and UA on the PANI-GO nanocomposite modified electrode shows rapid response of three well defined peaks with larger peak potential separation. Therefore, an electrochemical sensor for individual or simultaneous determination of these three biomolecules on PANI-GO/GCE can be achieved with higher sensitivity and selectivity. Thus PANI-GO nanocomposite with unique structural and electrocatalytic properties is a promising candidate for the fabrication of sensitive and selective biosensors.

References

- U. Yogeswaran, S. Thiagarajan and S. M. Chen, *Anal. Biochem.*, 2007, **365**, 122.
- D. Han, T. Han, C. Shan, A. Ivaska and L. Niu, *Electroanalysis*, 2010, **22**, 2001.
- J. Ping, J. Wu, Y. Wang and Y. Ying, *Biosens. Bioelectron.*, 2012, **34**, 70.
- Y. Zhang, R. Yuan, Y. Chai, W. Li, X. Zhong and H. Zhong, *Biosens. Bioelectron.*, 2011, **26**, 3977.
- M. Mallesha, R. Manjunatha, C. Nethravathi, G. S. Suresh, M. Rajamathi, J. S. Melo and T. V. Venkatasha, *Biochemistry*, 2011, **81**, 104.
- A. Bossi, S. A. Piletsky, E. V. Piletska, P. G. Righetti and A. P. F. Turner, *Anal. Chem.*, 2000, **72**, 4296.
- R. M. Wightman, L. J. May and A. C. Micheal, *Anal. Chem.*, 1998, **60**, 769A.
- M. Heinig and R. J. Johnson, *Cleveland Clin. J. Med.*, 2006, **73**, 1059.
- X. H. Lin, Y. F. Zhang, W. Chen and P. Wu, *Sens. Actuators, B*, 2007, **122**, 309.
- R. Zhang, G. D. Jin, D. Chen and X. Y. Hu, *Sens. Actuators, B*, 2009, **138**, 174.
- S. Y. Zhu, H. J. Li, W. X. Niu and G. B. Xu, *Biosens. Bioelectron.*, 2009, **25**, 940.
- C. Xiao, X. Chu, Y. Yang, X. Li, X. Zhang and J. Chen, *Biosens. Bioelectron.*, 2011, **26**, 2934.
- M. Noroozifar, M. K. Motlagh, R. Akbari and M. B. Parizi, *Biosens. Bioelectron.*, 2011, **28**, 56.

- 14 Y. Bao, J. Song, Y. Mao, D. Han, F. Yang, L. Niu and A. Ivaska, *Electroanalysis*, 2011, **23**, 878.
- 15 N. G. Deshpandle, Y. G. Gudage, R. Sharma, J. C. Vyas, J. B. Kim and Y. P. Lee, *Sens. Actuators, B*, 2009, **138**, 76.
- 16 Y. S. Negi and P. V. Adhyapak, *J. Macromol. Sci., Part C*, 2002, **42**, 35.
- 17 A. Rahy and D. J. Yang, *Mater. Lett.*, 2008, **62**, 4311.
- 18 D. M. Delongchamp and P. T. Hammond, *Chem. Mater.*, 2004, **16**, 4799.
- 19 A. J. Heeger, *Synth. Met.*, 2001, **125**, 23.
- 20 R. Mazeikiene, A. Statino, Z. Kuodis, G. Niaura and A. Malinauskas, *Electrochem. Commun.*, 2006, **8**, 1082.
- 21 I. G. Casella and M. R. Guascito, *Electroanalysis*, 1997, **9**, 1381.
- 22 Z. Wang, S. Liu, P. Wu and C. Cai, *Anal. Chem.*, 2009, **81**, 1638.
- 23 J. Mathiyarasu, S. Senthilkumar, K. L. N. Phani and V. Yegnaraman, *J. Appl. Electrochem.*, 2005, **35**, 513.
- 24 X. Feng, C. Mao, G. Yang, W. Hou and J. J. Zhu, *Langmuir*, 2006, **22**, 4384.
- 25 S. R. Ali, Y. Ma, R. R. Parajuli, Y. Balogum, W. Y. C. Lai and H. He, *Anal. Chem.*, 2007, **79**, 2583.
- 26 H. Hu, X. Wang, F. Liu, J. Wang and C. Xu, *Synth. Met.*, 2011, **161**, 404.
- 27 Y. Zhu, S. Murali, W. Cai, X. Li, J. W. Suk, J. R. Potts and R. S. Ruoff, *Adv. Mater.*, 2010, **22**, 3906.
- 28 P. Avouris, Z. Chen and V. Perebeinos, *Nat. Nanotechnol.*, 2007, **2**, 605.
- 29 S. R. C. Vivekchand, C. S. Rout, K. S. Subrahmanyam, A. Govindaraj and C. S. R. J. Rao, *J. Chem. Sci.*, 2008, **120**, 9.
- 30 Z. M. Ao, J. Yang, S. Lee and Q. Jiang, *Chem. Phys. Lett.*, 2008, **461**, 276.
- 31 Y. Wang, Y. M. Li, L. H. Tang, J. Lu and J. H. Li, *Electrochem. Commun.*, 2009, **11**, 889.
- 32 X. Kang, J. Wang, H. Wu, I. A. Aksay, J. Liu and Y. Lin, *Biosens. Bioelectron.*, 2009, **25**, 901.
- 33 W. J. Lin, C. S. Liao, J. H. Jhang and Y. C. Tsai, *Electrochem. Commun.*, 2009, **11**, 2153.
- 34 L. Wu, L. Feng, J. Ren and X. Qu, *Biosens. Bioelectron.*, 2012, **34**, 57.
- 35 H. Wang, Q. Hao, X. Yang, L. Lu and X. Wang, *ACS Appl. Mater. Interfaces*, 2010, **2**, 821.
- 36 H. Wang, Q. Hao, X. Yang, L. Lu and X. Wang, *Electrochem. Commun.*, 2009, **11**, 1158.
- 37 D. W. Wang, F. Li, J. Zhao, W. Ren, Z. G. Chen, J. Tan, Z. S. Wu, I. Gentle, G. Q. Lu and H. M. Cheng, *ACS Nano*, 2009, **3**, 1745.
- 38 K. Zhang, L. L. Zhang, X. S. Zhao and J. Wu, *Chem. Mater.*, 2010, **22**, 1392.
- 39 H. Bai, Y. Xu, L. Zhao, C. Li and G. Shi, *Chem. Commun.*, 2009, 1667.
- 40 G. L. Chen, S. M. Shau, T. Y. Juang, R. H. Lee, C. P. Chen, S. Y. Suen and R. J. Jeng, *Langmuir*, 2011, **27**, 14563.
- 41 P. Manivel, S. Ramakrishnan, N. K. Kothurkar, N. Ponpandian, D. Mangalaraj and C. Viswanathan, *J. Exp. Nanosci.*, 2013, **8**, 311.
- 42 Y. Liu, R. Deng, Z. Wang and H. Liu, *J. Mater. Chem.*, 2012, **22**, 13619.
- 43 Z. Gu, C. Li, G. Wang, L. Zhang, X. Li, W. Wang and S. Jin, *J. Polym. Sci., Part B: Polym. Phys.*, 2010, **48**, 1329.
- 44 L. A. Mashat, K. Shin, K. K. Zadeh, J. D. Plessis, S. H. Han, R. W. Kojima, R. B. Kaner, D. Li, X. Gou, S. J. Ippolito and W. Wlodarski, *J. Phys. Chem. C*, 2010, **114**, 16168.
- 45 A. Z. Sadek, W. Wlodarski, K. K. Zadeh, C. Baker and R. B. Kaner, *Sens. Actuators, A*, 2007, **139**, 53.
- 46 J. Yan, T. Wei, B. Shao, Z. Fan, W. Qian, M. Zhang and F. Wei, *Carbon*, 2010, **48**, 487.
- 47 C. Y. Yang, M. Reghu, A. J. Heeger and Y. Cao, *Synth. Met.*, 1996, **79**, 27.
- 48 P. Manivel, S. Ramakrishnan, N. K. Kothurkar, A. Balamurugan, N. Ponpandian, D. Mangalaraj and C. Viswanathan, *Mater. Res. Bull.*, 2013, **48**, 640.
- 49 Y. G. Wang, H. Q. Li and Y. Y. Xia, *Adv. Mater.*, 2006, **18**, 2619.
- 50 J. Ping, J. Wu, Y. Wang and Y. Ying, *Biosens. Bioelectron.*, 2012, **34**, 70.
- 51 A. Safavi, N. Maleki, O. Moradlou and F. Tajabadi, *Anal. Biochem.*, 2006, **359**, 224.
- 52 Z. H. Sheng, X. Q. Zheng, J. Y. Xu, W. J. Bao, F. B. Wang and X. H. Xia, *Biosens. Bioelectron.*, 2012, **34**, 125.